Cell Death & Differentiation (2021) 28:1466–1476
https://doi.org/10.1038/s41418-020-00673-z

Cell Death & Differentiation

ARTICLE

Necroptosis is dispensable for the development of inflammation-associated or sporadic colon cancer in mice

Silvia Alvarez-Diaz[1,2] · Adele Preaudet[1] · Andre L. Samson[1,2] · Paul M. Nguyen[1,2] · Ka Yee Fung[1,2] · Alexandra L. Garnham[1,2] · Warren S. Alexander[1,2] · Andreas Strasser[1,2] · Matthias Ernst[3] · Tracy L. Putoczki[1,2] · James M. Murphy[1,2]

Received: 17 April 2020 / Revised: 4 November 2020 / Accepted: 4 November 2020 / Published online: 23 November 2020

Abstract

Chronic inflammation of the large intestine is associated with an increased risk of developing colorectal cancer (CRC), the second most common cause of cancer-related deaths worldwide. Necroptosis has emerged as a form of lytic programmed cell death that, distinct from apoptosis, triggers an inflammatory response. Dysregulation of necroptosis has been linked to multiple chronic inflammatory diseases, including inflammatory bowel disease and cancer. Here, we used murine models of acute colitis, colitis-associated CRC, sporadic CRC, and spontaneous intestinal tumorigenesis to investigate the role of necroptosis in these gastrointestinal pathologies. In the Dextran Sodium Sulfate-induced acute colitis model, in some experiments, mice lacking the terminal necroptosis effector protein, MLKL, or its activator RIPK3, exhibited greater weight loss compared to wild-type mice, consistent with some earlier reports. However, the magnitude of weight loss and accompanying inflammatory pathology upon *Mlkl* deletion varied substantially between independent repeats. Such variation provides a possible explanation for conflicting literature reports. Furthermore, contrary to earlier reports, we observed that genetic deletion of MLKL had no impact on colon cancer development using several mouse models. Collectively, these data do not support an obligate role for necroptosis in inflammation or cancer within the gastrointestinal tract.

Introduction

Colorectal cancer (CRC) is one of the leading causes of cancer-related deaths worldwide [1]. Despite the significant progress in our understanding of the familial basis of this disease, genetic predisposition only accounts for ~20% of CRC cases [2]. Chronic inflammation is recognised as a critical factor in the progression of CRC following the observation that patients with inflammatory bowel disease (IBD) have an increased risk of CRC development [3], and the finding that long-term treatment with nonsteroidal anti-inflammatory drugs reduces the risk of CRC development [4]. While these observations highlight that the initiation and progression of CRC do not depend solely on the oncogenic mutations intrinsic to the neoplastic cells, we do not yet fully understand the complex mechanisms that regulate tumor-associated inflammatory responses.

Necroptosis is a lytic form of programmed cell death that is thought to have emerged as a host defense mechanism against infectious pathogens, particularly those that encode inhibitors of apoptosis [5–9]. Of note, the dysregulation of necroptosis has been implicated in the pathology of a range

These authors contributed equally: Tracy L. Putoczki, James M. Murphy

Edited by T. Mak

Supplementary information The online version of this article (https://doi.org/10.1038/s41418-020-00673-z) contains supplementary material, which is available to authorized users.

✉ Tracy L. Putoczki
putoczki.t@wehi.edu.au

✉ James M. Murphy
jamesm@wehi.edu.au

[1] The Walter and Eliza Hall Institute of Medical Research, Parkville, VIC 3052, Australia

[2] Department of Medical Biology, University of Melbourne, Parkville, VIC 3050, Australia

[3] Olivia Newton-John Cancer Research Institute, and La Trobe University School of Cancer Medicine, Heidelberg, VIC 3084, Australia

of inflammatory diseases [10–14]. Necroptotic signaling is induced downstream of activation of TNFR1, other death receptors, Toll-like receptors, interferon receptors, or certain DNA binding proteins (e.g., ZBP1) via three key effector proteins: the receptor-interacting serine/threonine protein kinases (RIPK)-1 [15, 16] and RIPK3 [5, 17, 18], and the mixed lineage kinase domain-like (MLKL) pseudokinase [19–23]. In scenarios where RIPK1 is not ubiquitylated by the cellular Inhibitors of Apoptosis Proteins [24, 25] or cleaved by caspase-8 [26, 27], it can nucleate the assembly of a high molecular weight signaling platform termed the "necrosome" with the RIPK3 kinase. Within this complex, RIPK3 can be activated by trans-phosphorylation [5], which leads to recruitment of the terminal effector in the pathway, the MLKL pseudokinase [9, 21]. RIPK3 phosphorylation of MLKL facilitates the assembly and plasma membrane translocation of MLKL oligomers [20, 28–33], which permeabilize membranes to induce lytic cell death [33, 34]. Unlike apoptosis, which is typically considered to be immunologically silent, necroptotic cell death provokes the release of damage-associated molecular patterns into the extracellular space thereby triggering an immune response [35]. While necroptotic cell death has been widely implicated as a driver of multiple human inflammatory diseases, including inflammation-associated cancers, many attributions remain controversial [12, 36].

In Crohn's Disease (CD) and Ulcerative Colitis (UC) patients, RIPK1, RIPK3, and MLKL expression are abnormally elevated in the diseased tissue [37, 38], suggesting that necroptosis may contribute to morbidity. Previous studies have shown that systemic, or intestinal epithelial specific, loss of RIPK1 resulted in the sporadic development of intestinal inflammation in mice [14, 39, 40], while conflicting results have been reported from studies using *Ripk3*-deficient mice. Some reported that loss of RIPK3 exacerbated DSS-induced acute colitis [41] and enhanced AOM/DSS induced inflammation-associated CRC [42], but others observed no overt phenotype in the DSS-induced acute colitis model [12]. The basis for these differences is not known but might be attributable to differences in experimental conditions, or a focus on pathology within specific subcompartments of the GI tract.

While the involvement of RIPK3 in these pathologies is debated, a role for RIPK3 might also reflect non-necroptotic functions, perhaps related to its role in the production of proinflammatory cytokines and chemokines [43, 44]. Accordingly, recent work has examined whether MLKL, the terminal effector in necroptotic signaling with known functions restricted to this pathway, is crucial to acute colitis and the development of colon cancer. Nevertheless, similar to studies with *Ripk3*$^{-/-}$ mice, those using *Mlkl*$^{-/-}$ mice have led to conflicting conclusions following DSS exposure, with exacerbation of [45] and protection from [46] colon inflammation reported by different groups. Consequently, the precise roles, if any, of the necroptosis effector, MLKL, and its activator, RIPK3, in colonic inflammation and tumorigenesis remain unclear.

Discordant findings in previous studies may have arisen from the focus on individual aspects of GI pathology, and comparisons of necroptosis-deficient non-littermates and/or non-cohoused control mice. Here, we sought to resolve these discrepancies by investigating the contribution of necroptotic cell death to gastrointestinal (GI) pathologies through comparison of *Ripk3*$^{-/-}$ as well as *Mlkl*$^{-/-}$ mice with their respective littermates in an acute colitis inflammatory model, and complementary cancer models encompassing colitis-associated CRC, sporadic CRC, and spontaneous intestinal tumorigenesis. Our data indicate that colonic inflammation in DSS-induced acute colitis can occur independently of the RIPK3-MLKL necroptotic signaling axis. It is notable that we observed substantial heterogeneity between the burden of inflammation in independent repeat experiments in this model. Such variability between independent studies, even when conducted in the same animal facility and by the same experimenters, may reconcile the conflicting attributions of necroptotic death in promotion or attenuation of GI inflammation in previous reports. Furthermore, loss of neither *Mlkl* nor *Ripk3* impacted tumor development, indicating that necroptosis does not play a substantive role in several murine models of colon cancer.

Results

Mlkl$^{-/-}$ and *Ripk3*$^{-/-}$ mice exhibited increased weight loss compared to wild-type littermates during a model of acute colitis

To understand the impact of loss of *Mlkl* on the extent of acute dextran sulfate sodium (DSS)-induced mucosal damage, we compared susceptibility between *Mlkl*$^{-/-}$ and littermate wild-type mice directly to *Ripk3*$^{-/-}$ mice. MLKL is the terminal known effector in the necroptosis pathway, and unlike RIPK3, does not have additional functions in apoptotic signaling [47, 48] or driving inflammatory cytokine and chemokine production [43, 44]. Accordingly, we focused our study on *Mlkl*$^{-/-}$ mice to examine the precise role of necroptotic cell death in DSS-induced pathology. We included a *Ripk3*$^{-/-}$ cohort, albeit not matched with littermate wild-type control mice, as a comparator, because this strain has been widely studied by others in this model. The mucosa of the distal colon (DC) was assessed by endoscopy prior to administration of DSS, and as colitis developed on days 5 and 8 of the challenge (Fig. 1a). We observed no significant difference in the murine endoscopic index of colitis (MEIC) scores [49] between the three

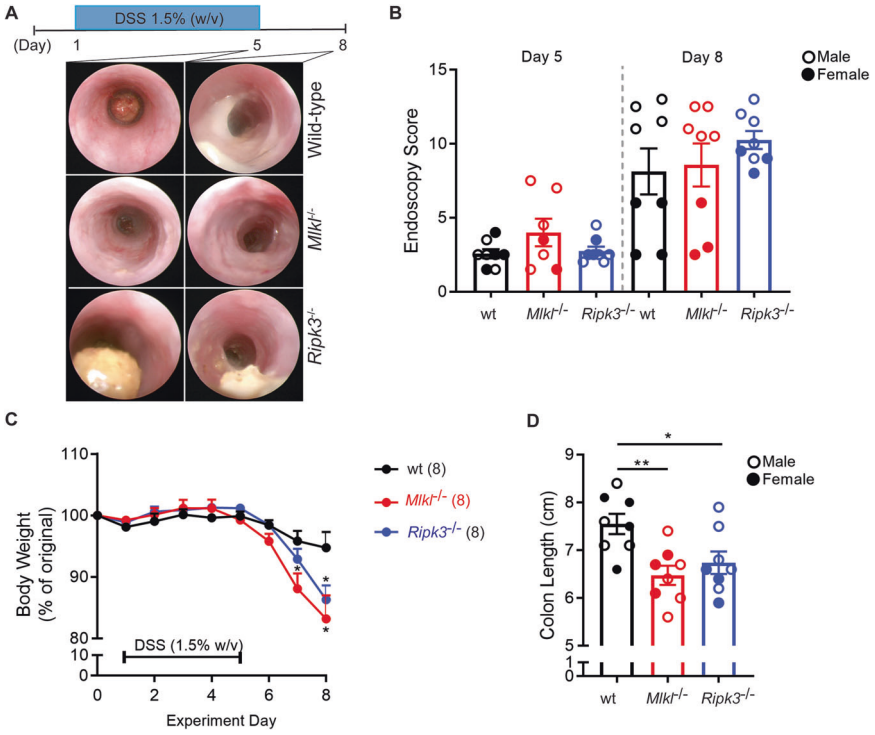

Fig. 1 Loss of MLKL or RIPK3 results in increased weight loss in a mouse model of colitis, but only in some cohorts. a Schematic illustration of the DSS-induced acute colitis model with representative endoscopy images of mice of the indicated genotypes. **b** Serial murine endoscopic index of colitis (MEIC) scores for mice of the indicated genotypes on day 5 and day 8 of the DSS-induced acute colitis model. Littermate wild-type mice ($Mlkl^{+/+}$) were used as controls. $N = 8$ mice per genotype. Data are presented as mean ± SEM. Male and female mice are indicated. There is no significant difference between genotypes or sexes on Day 5 (power of 0.413). There is no significant difference between male mice on Day 8; for female mice wt vs $Ripk3^{-/-}$ mice $^*p = 0.02$, $Mlkl^{-/-}$ vs $Ripk3^{-/-}$ mice $^*P = 0.02$ (ANOVA, power of 0.181). **c** Daily weight loss, presented as a percentage of the starting weight, for mice of the indicated genotypes. $N = 8$ mice per genotype. Data are presented as mean ± SEM. $^*P < 0.05$, Student's unpaired t test, power of 0.347. **d** Colon length for mice of the indicated genotypes. $N = 8$ mice per genotype. Data are presented as mean ± SEM. $^*P < 0.05$, $^{**}P < 0.01$, Student's unpaired t test. Male and female mice are indicated. There are significant differences between female wt vs $Ripk3^{-/-}$ mice $^*p = 0.04$ (t test, power of 0.665), and between male wt vs $Mlkl^{-/-}$ mice $^*p = 0.04$ (t test, power of 0.926).

genotypes at these time points (Fig. 1b). However, when animals were returned to normal drinking water for 3 days, following administration of DSS for 5 days, to enable mucosal recovery, both $Mlkl^{-/-}$ and $Ripk3^{-/-}$ mice displayed significantly increased weight loss compared to the wild-type mice, suggesting increased clinical symptoms of colitis (Fig. 1c). In line with this, a significant reduction in colon length was observed in $Mlkl^{-/-}$ and $Ripk3^{-/-}$ mice on autopsy compared to $Mlkl^{+/+}$ (wild-type) littermates (Fig. 1d). It is noteworthy that this phenotype is not fully penetrant, and when these experiments were performed with non-littermate controls, the changes in weight loss or colon length remained similar (Supplementary Fig. 1A, B). These findings prompted us to examine susceptibility of a further cohort of wild-type and $Mlkl^{-/-}$ littermates to DSS-induced colitis (Supplementary Fig. 1D, E). We observed a trend toward greater weight loss in the $Mlkl^{-/-}$ mice (Supplementary Fig. 1D), consistent with our initial littermate study (Fig. 1b), but contrastingly a trend toward longer colon length among the $Mlkl^{-/-}$ mice. Thus, in this model, loss of MLKL or RIPK3 do not exert reproducible impact on morbidity.

MLKL and RIPK3 are dispensable for inducing inflammation during acute colitis

To determine whether $Mlkl^{-/-}$ and $Ripk3^{-/-}$ mice exhibited changes in mucosal architecture, hematoxylin and eosin (H&E) stained sections of Swiss rolls of the entire colon from mice of the above described studies were examined (Fig. 2a; Supplementary Fig. 1C). We compared epithelial damage in the proximal colon (PC), middle colon (MC), and DC, and observed that the majority of mucosal damage occurred in the DC in this model (Fig. 2b). The more profound damage in the DC compared to the PC arises because of greater susceptibility to DSS, which can be attributed to distinct physiological roles [50], cytokine and immune cell gradients [51] of the colon subcompartments. While mice of all genotypes exhibited histopathological signs of mucosal damage, we found no significant differences in any region

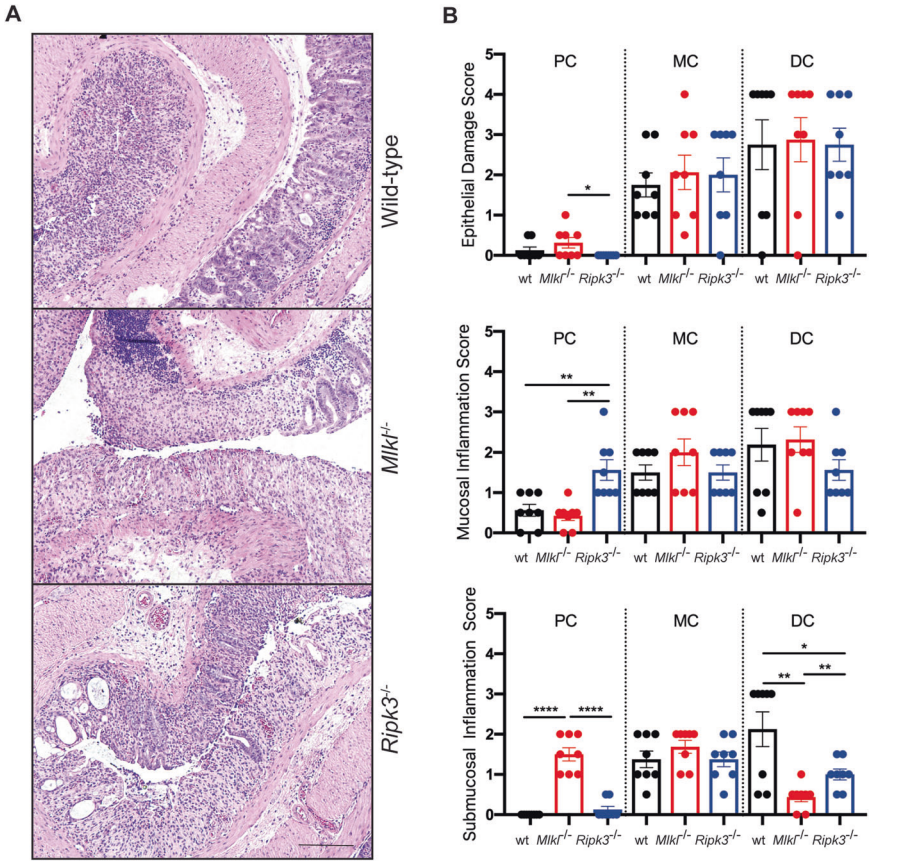

Fig. 2 Loss of MLKL or RIPK3 decreases submucosal inflammation in a model of colitis. a Representative H&E-stained sections from swiss rolls of colons from mice of the indicated genotypes at the conclusion of the experiment. Scale bar: 100 µm. **b** Histological scoring of epithelial damage, mucosal inflammation and submucosal inflammation from mice of the indicated genotypes. $N = 8$ mice per genotype. Data are presented as mean ± SEM. $^{*}P < 0.05$, $^{**}P < 0.01$, $^{****}P < 0.0001$. Student's unpaired t test.

of the colon when comparing *Ripk3*$^{-/-}$ or *Mlkl*$^{-/-}$ mice to the wild-type mice. This indicates that loss of MLKL or RIPK3 do not enhance retention of crypt architecture in this model (Fig. 2b). Similarly, we found comparable mucosal inflammation between mice of the different genotypes, with the exception of the PC, where a significant increase in mucosal inflammation was observed in the *Ripk3*$^{-/-}$ mice (Fig. 2b). These observations are consistent with the lack of difference in the MEIC scores for the DC between mice of the different genotypes (Fig. 1b). In this experiment, the most striking histological differences were observed in the submucosa, where *Mlkl*$^{-/-}$ mice had significantly increased inflammation in the PC compared to their wild-type littermates, while inflammation in the DC was decreased, similar to the *Ripk3*$^{-/-}$ mice (Fig. 2b). Our observation that the extent of weight loss and colon length varied substantially within mice of a given genotype between experiments (Supplementary Fig. 1D, E) led us to further examine whether this variably was reflected in inflammatory pathology. Indeed, histological examination of wild-type and *Mlkl*$^{-/-}$ mice—both in a nonlittermate and a second littermate cohort study (Supplementary Fig. 1C, F)—supported the idea that necroptosis-deficient mice exhibit variable inflammatory responses in the DSS-induced acute colitis model. This indicates a nonobligate role for necroptosis in this model. To further explore this observation, serum levels of the proinflammatory cytokine Interleukin (IL)-6 were examined (Supplementary Fig. 2), with no significant changes observed between mice of the different genotypes. Furthermore, the observed inter-experimental variability in phenotype suggests a possible basis for the contrary literature reports on the role for necroptotic death in colitis protection or exacerbation.

MLKL or RIPK3 deficiency do not alter the development of colitis-associated cancer

To assess a potential contribution of necroptosis to inflammation-associated cancers, we directly compared the influence of loss of RIPK3 or MLKL on the onset and progression of colitis-associated cancer. On day 1 of the colitis-associated cancer model, a single injection of the alkylating mutagen azoxymethane (AOM) was administered to wild-type and *Mlkl*$^{-/-}$ littermate mice, as well as *Ripk3*$^{-/-}$ mice, to induce amongst other errors, sporadic missense mutations in the *Ctnb1* gene in colonic epithelial cells [52, 53] (Fig. 3a). Cyclic oral administration of the luminal irritant DSS was provided via drinking water on days 8–13 following AOM

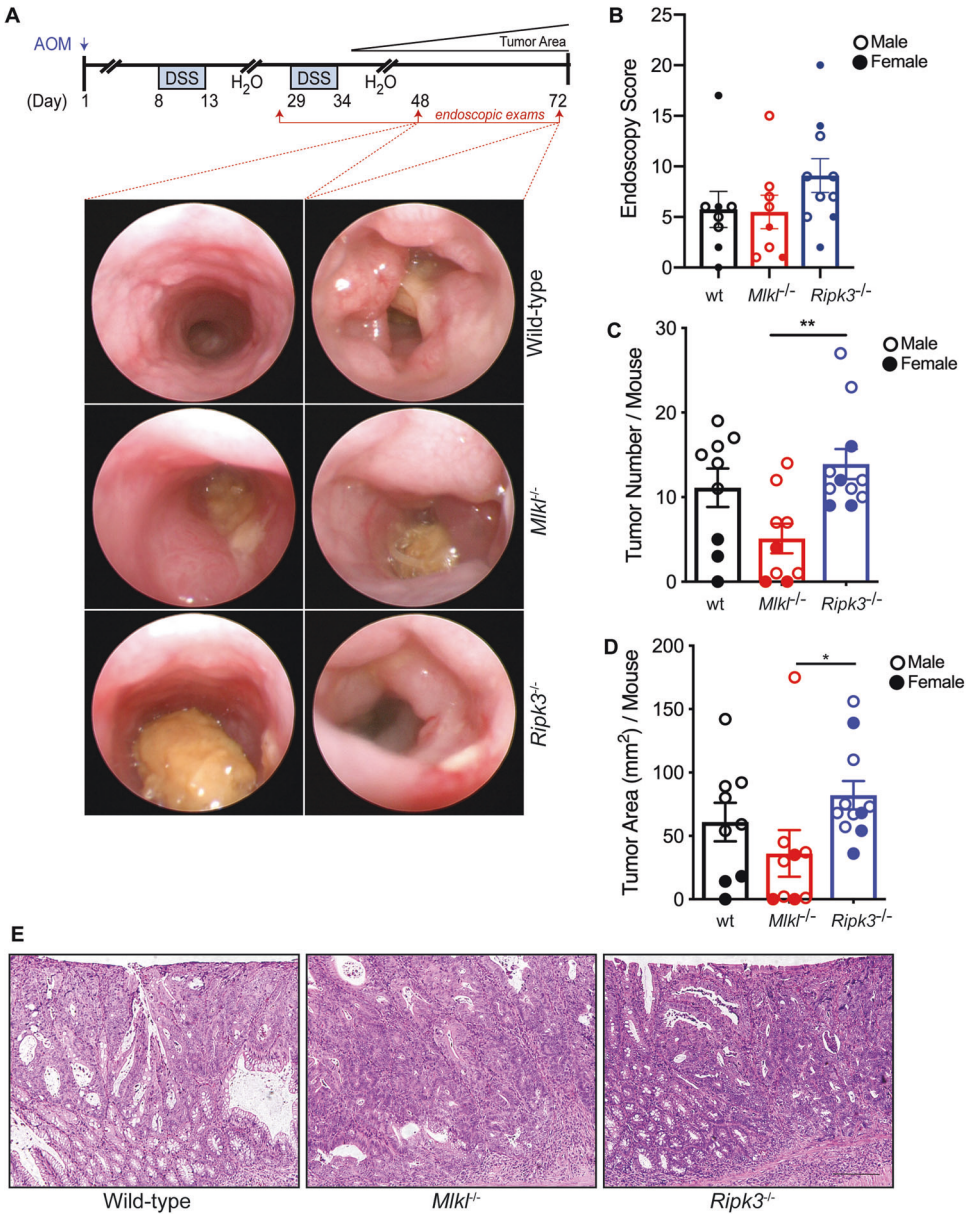

Fig. 3 Loss of MLKL or RIPK3 has no impact on the development of colitis-associated cancer. a Schematic illustration of the colitis-associated cancer model with representative endoscopy images of mice of the indicated genotypes. **b** Endoscopic tumor scores at the end of the colitis-associated cancer model for mice of the indicated genotypes. Littermate wild-type mice ($Mlkl^{+/+}$) were used as controls. $N > 9$ mice per genotype. Male and female mice are indicated. Data are presented as mean ± SEM. Student's unpaired *t* tests were applied to test for significant differences between wt vs $Ripk3^{-/-}$ (power 0.260), wt vs $Mlkl^{-/-}$ (power 0.051), and $Ripk3^{-/-}$ vs $Mlkl^{-/-}$ (power 0.307). **c** Tumor number at autopsy for mice of the indicated genotype. Littermate wild-type mice ($Mlkl^{+/+}$) were used as controls. $N > 9$ mice per genotype. Data are presented as mean ± SEM. $^{**}P < 0.01$. Student's unpaired *t* test. Male and female mice are indicated. There are significant differences between female wt vs $Ripk3^{-/-}$ mice $^{*}p = 0.01$ (*t* test), and $Mlkl^{-/-}$ vs $Ripk3^{-/-}$ mice $^{**}p = 0.006$ (*t* test). There are significant differences between male wt vs $Mlkl^{-/-}$ mice $^{**}p = 0.007$ (*t* test), and $Mlkl^{-/-}$ vs $Ripk3^{-/-}$ mice $^{*}p = 0.04$ (*t* test). The power of the wt vs $Ripk3^{-/-}$ test is 0.164, wt vs $Mlkl^{-/-}$ is 0.493, and $Mlkl^{-/-}$ vs $Ripk3^{-/-}$ is 0.909. **d** Tumor burden at autopsy for mice of the indicated genotypes. Littermate wild-type mice ($Mlkl^{+/+}$) were used as controls. $N > 9$ mice per genotype. Data are presented as mean ± SEM. Male and female mice are indicated. There are significant differences between $Mlkl^{-/-}$ vs $Ripk3^{-/-}$ mice $^{*}p = 0.04$ (*t* test). The power of the wt vs $Ripk3^{-/-}$ test is 0.193, wt vs $Mlkl^{-/-}$ is 0.165, and $Mlkl^{-/-}$ vs $Ripk3^{-/-}$ is 0.556. **e** Representative images of H&E stained sections of tumors in the distal colon from mice of the indicated genotypes at the conclusion of the experiment. Scale bar: 100 µm.

administration, followed by 16 days of normal drinking water and a further 5 days of DSS via drinking water to induce 'flares' of acute inflammation, similar to that observed in UC patients. This treatment ultimately promotes the development of tumors in the DC of mice [54]. As per ethical requirements, all animals were weighed daily with no significant differences

in weight loss observed between the genotypes (Supplementary Fig. 3A).

Serial endoscopic monitoring of colitis-associated cancer mice revealed similar timing of tumor onset (Fig. 3a) and overall tumor burden (Fig. 3b) between mice of the different genotypes. This was further apparent on autopsy, where overall colonic tumor number (Fig. 3c) and burden (Fig. 3d) were comparable between the genotypes, with the exception of an increased tumor number in *Ripk3*$^{-/-}$ compared to *Mlkl*$^{-/-}$ mice. The only macroscopic difference between mice of the different genotypes was a significant reduction in the colon length in *Ripk3*$^{-/-}$ mice compared to wild-type mice (Supplementary Fig. 3B). There were no visible changes to the influx of inflammatory cells in the tumors of the different mouse genotypes (Fig. 3e). We validated MLKL and RIPK3 expression in colonic tumor tissue by Western blot analysis. This revealed mildly increased MLKL and RIPK3 expression in the tumor compared to normal tissue of wild-type mice (Supplementary Fig. 3C). As expected, we observed no MLKL or RIPK3 signals in tissues sourced from *Mlkl*$^{-/-}$ and *Ripk3*$^{-/-}$ mice, respectively. To validate this observation, a second experiment comparing wild-type and *Mlkl*$^{-/-}$ mice was performed (Supplemental Fig. 4), which confirmed the lack of a clear phenotype. We also examined the level of IL-6 in lysates from non-tumor and tumor tissues (Supplementary Fig. 5A). We found no significant difference in IL-6 expression levels, suggesting comparable inflammation. While MLKL and RIPK3 are present in tumor tissue, our results suggest that elevations in their expression neither predisposes the colon to, nor contributes to, colon-associated cancer onset or progression in this model.

MLKL or RIPK3 is dispensable for the development of sporadic colon cancer

We next sought to determine if there was a tumor suppressive function for MLKL in sporadic cancer models associated with an inflammatory tumor microenvironment that was not triggered by mucosal damage. To this end, we induced colonic tumors by injecting wild-type mice and littermate *Mlkl*$^{-/-}$ mice, as well as *Ripk3*$^{-/-}$ mice with AOM once weekly over 6 weeks and aged the animals for up to 280 days after the last injection to allow for the accumulation of mutagenic events in the colonic epithelium (Fig. 4a). Tumor initiation was monitored by serial endoscopy. Upon autopsy, no significant differences in colonic tumor number (Fig. 4b) or overall tumor burden (Fig. 4c) could be observed between the different genotypes. As with the colitis-associated cancer model, no overt differences in inflammation were observed in the tumors of mice from any genotype (Fig. 4d). We also examined the level of IL-6 in lysates from non-tumor and tumor tissues (Supplementary Fig. 5B) and found no significant difference in the expression levels of this cytokine. The levels of IL-6 were very low, as anticipated for a non-inflammation driven, mutagen-induced sporadic CRC model. Western blot analysis suggested increased RIPK3 levels in colonic tumors compared to normal tissue of wild-type mice. However, no substantive corresponding increase in MLKL was observed (Supplementary Fig. 6). Collectively, our results suggest that the RIPK3-MLKL necroptosis axis does not contribute to sporadic colon cancer development.

Because RIPK3 [12] and MLKL [55] have been shown to be highly expressed in the small intestine, we explored the contribution of necroptotic signaling to tumors in this region of the GI tract by crossing *Mlkl*$^{-/-}$ mice to *Apc*$^{min/+}$ mice, which carry a heterozygous germline truncation mutation in the *Apc* tumor suppressor gene. Following spontaneous loss-of-heterozygosity of the remaining wild-type *Apc* allele and the resultant aberrant WNT pathway signaling, *Apc*$^{min/+}$ mice develop spontaneous tumors in the small intestine [56]. We aged *Mlkl*$^{-/-}$;*Apc*$^{min/+}$ compound mutant mice and littermate *Apc*$^{min/+}$ mice to 90, 100, and >130 days (Fig. 5a). Notably, we observed no significant difference in the overall macroscopic tumor number (Fig. 5b) or tumor burden (Fig. 5c) in the proximal (PSI), middle (MSI), or distal small intestine (DSI) between the genotypes. We also observed no difference in the formation of sporadic tumors in the colon of *Mlkl*$^{-/-}$;*Apc*$^{min/+}$ mice compared to *Apc*$^{min/+}$ mice (Fig. 5b, c), consistent with our observations in the AOM model (Fig. 4). Collectively, these observations indicate that the loss of MLKL has no impact on sporadic tumor onset or progression in the small intestine or colon.

Discussion

While the terminal necroptosis effector, MLKL, and its activator RIPK3, are known to be highly expressed in the GI epithelium [12, 37, 38, 55, 57], the role of necroptotic cell death in GI pathologies has remained unclear. Studies using mice lacking RIPK3 or MLKL have led to conflicting observations in models of acute colitis and inflammation-induced colon cancer, with no overt phenotype [12], protection [46] or exacerbation [41, 42, 45] variously reported. Typically, prior studies have examined *Mlkl*$^{-/-}$ or *Ripk3*$^{-/-}$ mice individually, but not in parallel, and only seldom used littermates as controls [42], and with different levels of exposure to mucosal damaging agents (1.5–3.5% DSS for 5–7 days [12, 42]). Here, we sought to resolve these inconsistencies by comparing *Mlkl*$^{-/-}$ mice and wild-type littermate controls with *Ripk3*$^{-/-}$ mice in parallel to more precisely define the role for necroptosis in GI pathologies.

We used the acute DSS-induced mucosal damage model (5 days 1.5% w/v DSS, 3 days water) that mimics the epithelial damage characteristic of ulcerative colitis [49].

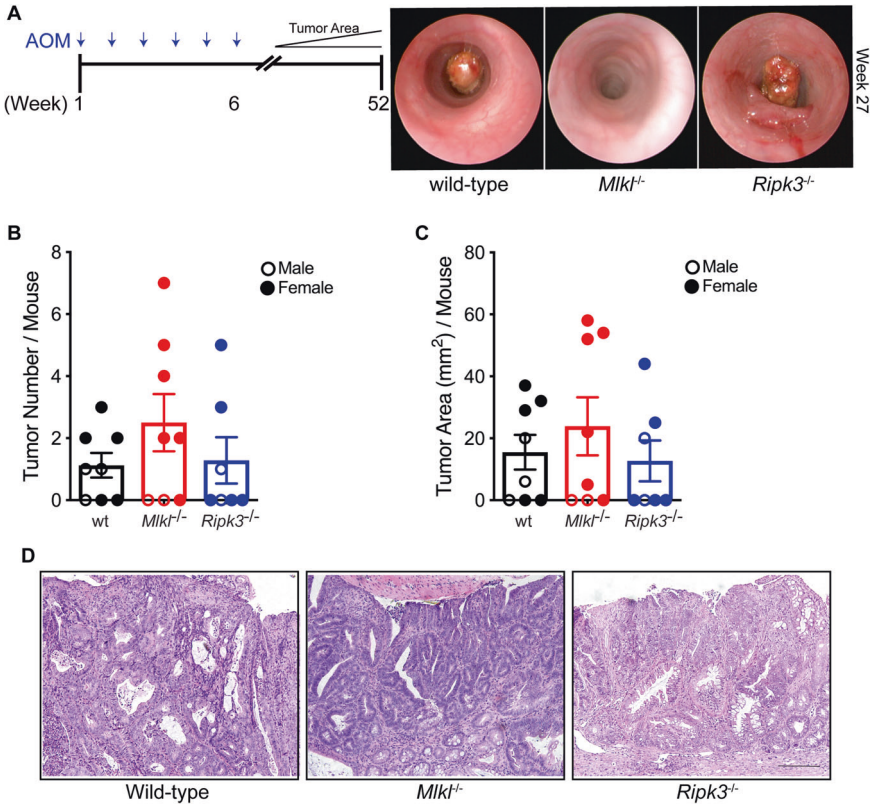

Fig. 4 Loss of MLKL or RIPK3 has no impact on sporadic colon cancer development. a Schematic illustration of the sporadic cancer model with representative endoscopy images of mice of the indicated genotypes. **b** Tumor number at autopsy for mice of the indicated genotypes. Littermate wild-type mice ($Mlkl^{+/+}$) were used as controls. $N > 8$ mice per genotype. Male and female mice are indicated, with no significant differences observed within each sex. Data are presented as mean ± SEM. The power of the wt vs $Ripk3^{-/-}$ test is 0.225, wt vs $Mlkl^{-/-}$ is 0.054, and $Mlkl^{-/-}$ vs $Ripk3^{-/-}$ is 0.138. **c** Tumor burden at autopsy for mice of the indicated genotypes. Littermate wild-type mice ($Mlkl^{+/+}$) were used as controls. $N > 9$ mice per genotype. Male and female mice are indicated, with no significant differences observed within each sex. Data are presented as mean ± SEM. The power of the wt vs $Ripk3^{-/-}$ test is 0.060, wt vs $Mlkl^{-/-}$ is 0.085, and $Mlkl^{-/-}$ vs $Ripk3^{-/-}$ is 0.114. **d** Representative tumor H&E-stained sections of the distal colon from mice of the indicated genotypes at the conclusion of the experiment. Scale bar: 100 µm.

In this model, weight loss and immune cell infiltration peak when the mice are provided normal water, which allowed us to monitor both epithelial and immune cell infiltration to mucosal damage in parallel. We observed increased weight loss in $Ripk3^{-/-}$ and $Mlkl^{-/-}$ mice relative to littermate controls. However, exacerbated colitis, as reflected by decreased colon lengths [49], was only evident in one of our experimental repeats using littermate wild-type control mice. This may suggest variable susceptibility to inflammatory pathologies among necroptosis-deficient mice. The heterogeneity amongst experimental cohorts was reflected in endoscopic monitoring as well as epithelial damage scores. Comparisons of pathological changes within all regions of the colon only implicated MLKL and RIPK3 in the submucosal immune response in the DC in only one experimental repeat using matched wild-type littermate controls. Taking all our data in consideration, they are most consistent with a nonobligate function for the necroptosis machinery in driving inflammation in the DSS-induced acute colitis model. It is important to note that the absence of effects caused by necroptosis effector knockout in the DSS-induced inflammation model and carcinogenesis models are not because of deficits in statistical power. The cohort sizes used in our study are comparable to those used in earlier studies with these models, and power calculations indicate that overall we have adequate power to detect statistically-significant differences if they were present in the data. Together with earlier studies of the impact of deficiency of necroptotic effectors in mouse models of disease [12, 58–60], our observations highlight the intrinsic inter-experiment variability in the DSS-induced acute colitis model. They underscore the importance of controlling for differences in commensal microflora, and the sexes and genetic background of mice when examining the contribution of the necroptosis machinery (or any other cellular pathway) to disease using this model.

Recently, pharmacological inhibition of RIPK1 kinase was reported to protect mice in the $CD4^{+}CD45RB^{high}$ T cell

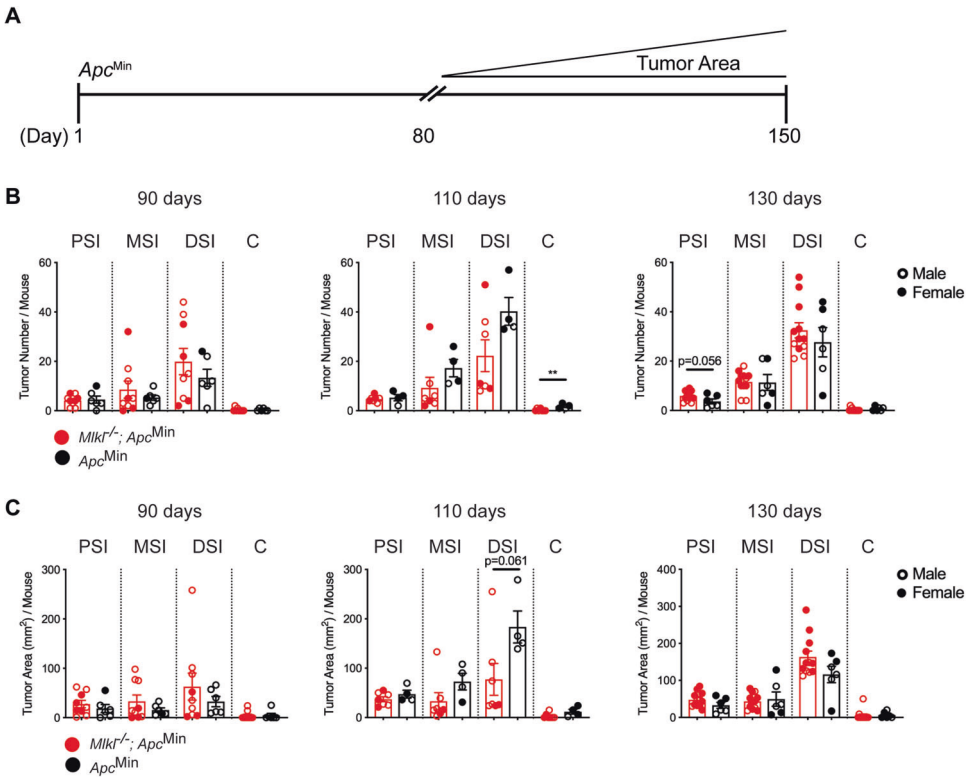

Fig. 5 Loss of MLKL does not impact tumor burden in the *Apc*^{min} model of intestinal adenomas. a Schematic illustration of tumor progression in the *Apc*^{min} mouse model of intestinal adenomas. **b** Adenoma number in mice of the indicated genotypes at ~90, 110, and >130 days of the age. Data are separated based on location within the intestine. Proximal Small Intestine (PSI), Middle Small Intestine (MSI), and colon (C). $N > 4$ mice per genotype. Male and female mice are indicated, with no significant differences observed within each sex. Data are presented as mean ± SEM. $^*P < 0.05$, Student's unpaired *t* test. Power of tests at 90 days for PSI is 0.157, MSI is 0.105, DSI is 0.136, and C is 0.050. Power of tests at 110 days for PSI is 0.072, MSI is 0.204, DSI is 0.384, and C is 0.861. Power for tests at 130 days for PSI is 0.491, MSI is 0.051, DSI is 0.118, and C is 0.207. **c** Adenoma burden in mice of the indicated genotypes at ~90, 110, and >130 days of the age. Data are separated based on location within the intestine. Proximal Small Intestine (PSI), Middle Small Intestine (MSI), and colon (C). $N > 4$ mice per genotype. Male and female mice are indicated, with no significant differences observed within each sex, with the exception of the PSI at 130 days, $^*P = 0.02$ (*t* test). Data are presented as mean ± SEM. $^*P < 0.05$, Student's unpaired *t* test. Power of tests at 90 days for PSI is 0.116, MSI is 0.169, DSI is 0.127, and C is 0.050. Power of tests at 110 days for PSI is 0.177, MSI is 0.272, DSI is 0.481, and C is 0.340. Power for tests at 130 days for PSI is 0.297, MSI is 0.064, DSI is 0.378, and C is 0.054.

transfer model of colitis [61], raising the prospect that necroptosis might contribute to the pathology of other models of colitis. However, because RIPK1 regulates not only necroptosis, but also proinflammatory and apoptosis signaling axes, whether the observed protection is attributable solely to blockade of necroptotic cell death and its consequences remains to be explored. Such examinations will have to rely on generation of MLKL-deficient mice on different genetic backgrounds, such as BALB/c, for application of the T-cell directed TNBS model of Crohn's disease, or the development of MLKL-selective inhibitors that are suitable for studies in mice of any genetic background.

We observed no role for RIPK3 or MLKL in multiple models of GI cancer that we have previously used in the study of apoptotic regulators [62]. Our findings differ from some previous reports [42, 63], although the use of littermates was not reported in these studies. This is an important consideration, because even small genetic differences, such as those between C57BL/6 J and C57BL/6NJ mouse strains, were reported to impact susceptibility of the latter to TNF- or LPS-induced sterile sepsis [64]. Each of the models that we employed are epithelial tumor models, driven by specific aberrations in the WNT-signaling pathway [49], which mimic the first step of CRC development in humans. Given the limited impact of loss of RIPK3 or MLKL in the acute-colitis model, it is reasonable to assume that the mutational burden in epithelial cells dominates the tumorigenic response. This would lead to enhanced epithelial cell proliferation and survival, which may outweigh any underlying immune role for MLKL in these cancer models. This does not preclude a role for MLKL in other GI cancers, with roles for inflammation in Gastrointestinal Stromal Tumors and neuroendocrine tumors not well characterized, and animal models for these cancers not well developed. Future studies will play an important role in illuminating which GI subcompartments are prone to necroptosis-induced

inflammation and the cell populations that underlie these phenotypes.

Materials and methods

Mice and treatments

All animal procedures were approved by and conducted in accordance with the Animal Ethics Committee of the Walter and Eliza Hall Institute, Australia. Mice lacking functional alleles for MLKL ($Mlkl^{-/-}$) [20] or RIPK3 ($Ripk3^{-/-}$) [65] or heterozygous for *Apc* ($Apc^{min/+}$) [56] have been described previously. All mice were bred on a C57BL/6 J genetic background. Wild-type littermate controls bred from $Mlkl^{+/-}$ crosses were used for comparison; *Ripk3*-deficient mice were maintained as, and bred from, $Ripk3^{-/-}$ homozygotes, rather than heterozygotes. To minimize variation in gut microflora, all animals were bred in the same room and housed on the same rack in a specific pathogen-free barrier facility at the Walter and Eliza Hall Institute, Australia. Animals were not randomized within genotype groups.

Acute DSS-induced colitis was elicited by providing drinking water *ad libitum* containing 1.5% DSS (w/v; MP Biomedicals, molecular weight 35,000–50,000 kDa) for 5 days, followed by 3 days of normal drinking water. Colitis-associated cancer was induced by intraperitoneal (i.p.) injection of AOM (10 mg/kg; Sigma). One week later, animals were provided drinking water *ad libitum* containing 2% DSS (w/v; MP Biomedicals, molecular weight 35,000–50,000 kDa) for 5 days, followed by 2 weeks of normal drinking water, which was repeated for two cycles as indicated. For studies on CRC development, animals received i.p. injections of AOM (10 mg/kg) once weekly over 6 consecutive weeks. Tumor onset and progression in the DC were monitored by endoscopy, with the investigator blinded, as described previously [66].

Tissue collection

At autopsy, colons were excised from the anus to the caecum and measured. Once opened longitudinally, tumors were enumerated according to their size. For the colon-associated cancer and CRC models, representative distal tumor and adjacent nontumor tissues were snap frozen. Swiss rolls of the entire small intestine or colon were prepared for histological processing.

Immunoblotting

Snap-frozen colon tissue samples were homogenized in ice-cold RIPA buffer (10 mM Tris-HCl (pH 8.0), 1 mM EGTA, 1 mM $MgCl_2$, 0.5% (v/v) Triton-X100, 0.1% (w/v) sodium deoxycholate, 0.5% (w/v) sodium dodecyl sulfate, 90 mM NaCl, 1x Protease/Phosphatase Inhibitor Cocktail (Cell Signaling Technology) and ~250 unit/mL Benzonase) with a stainless steel bead using a Qiagen TissueLyser II (1 min at 30 Hz). Homogenates were centrifuged (21,000 × *g*, 3 min, 4 °C) and the soluble protein concentration determined by using the bicinchoninic acid assay (Pierce). A total of 60 µg protein of each homogenate was subjected to SDS-PAGE (NuPAGE 4-12% Bis-Tris pre-cast gels; Life Technologies) and proteins were then transferred to PVDF membranes (Immobilon-FL; Millipore). Membranes were probed with primary antibodies (1 µg/mL) biotinylated monoclonal rat anti-mouse MLKL antibody (clone 3H1; [20] produced in-house), 1 µg/mL biotinylated monoclonal rat anti-mouse RIPK3 antibody (clone 8G7 [9]; produced in-house), mouse anti-GAPDH (Millipore; clone 6C5), then the corresponding secondary detection reagents (IRDye 800CW-conjugated streptavidin or IRDye 800CW-conjugated donkey anti-mouse IgG antibody; Licor) and the signal was visualized using an Odyssey Infrared Imaging System (LI-COR).

ELISA

Serum obtained from terminal cardiac bleeds, or tissue protein lysates, were analyzed using a mouse ELISA kit (Invitrogen) as per the manufacturer's instructions.

Statistical analysis

All data are presented as mean ± SEM and are representative of two or more experiments. Statistical significance was determined using a two-tailed Student's *t* test or ANOVA (parametric or non-parametric) with Bonferroni's post-hoc as appropriate. Power calculations were performed post-hoc using the R statistical programming language and the software packages pwr (version 1.3-0), pwr2 (version 1.0), WebPower (version 0.5.2), effsize (version 0.8.0), and effectsize (version 0.3.3).

Acknowledgements We thank Drs Kim Newton and Vishva Dixit (Genentech) for provision of the $Ripk3^{-/-}$ mouse strain. This project was funded by Cancer Council Victoria (1086419) with additional support from the National Health and Medical Research Council (NHMRC) of Australia (1113577, 1058344 to WSA; 461221, 1116937, 1113133, 1143105 to AS; 1124735, 1124737, 1105754, 1172929 to JMM) and a WEHI Dyson Bequest Centenary Fellowship (TLP), and Victorian Cancer Agency Fellowship (MCRF16009 to TLP). We gratefully acknowledge infrastructure support from the NHMRC IRIISS (9000587) and the Victorian State Government Operational Infrastructure Support Program.

Author contributions SAD, AS, TLP, and JMM conceived overall study. SAD, ALS, KYF designed and performed experiments and analyzed data. AP and PMN designed experiments, performed endoscopies, and analyzed data. ALG performed statistical analyses.

WSA generated mice, and together with AS and ME provided critical feedback. TLP designed experiments, analyzed data, prepared figures, and wrote the manuscript with JMM with input from AS.

Compliance with ethical standards

Conflict of interest ALS and JMM contribute to the development of necroptosis inhibitors in collaboration with Anaxis Pty Ltd.

Publisher's note Springer Nature remains neutral with regard to jurisdictional claims in published maps and institutional affiliations.

References

1. Rawla P, Sunkara T, Barsouk A. Epidemiology of colorectal cancer: incidence, mortality, survival, and risk factors. Prz Gastroenterol. 2019;14:89–103.
2. Rustgi AK. The genetics of hereditary colon cancer. Genes Dev. 2007;21:2525–38.
3. Stidham RW, Higgins PDR. Colorectal cancer in inflammatory bowel disease. Clin Colon Rectal Surg. 2018;31:168–78.
4. Burn J, Bishop DT, Chapman PD, Elliott F, Bertario L, Dunlop MG, et al. A randomized placebo-controlled prevention trial of aspirin and/or resistant starch in young people with familial adenomatous polyposis. Cancer Prev Res (Philos). 2011;4:655–65.
5. Cho YS, Challa S, Moquin D, Genga R, Ray TD, Guildford M, et al. Phosphorylation-driven assembly of the RIP1-RIP3 complex regulates programmed necrosis and virus-induced inflammation. Cell. 2009;137:1112–23.
6. Kitur K, Wachtel S, Brown A, Wickersham M, Paulino F, Penaloza HF, et al. Necroptosis promotes staphylococcus aureus clearance by inhibiting excessive inflammatory signaling. Cell Rep. 2016;16:2219–30.
7. Nailwal H, Chan FK. Necroptosis in anti-viral inflammation. *Cell Death Differ* 2019;26:4–13.
8. Pearson JS, Giogha C, Muhlen S, Nachbur U, Pham CL, Zhang Y, et al. EspL is a bacterial cysteine protease effector that cleaves RHIM proteins to block necroptosis and inflammation. Nat Microbiol. 2017;2:16258.
9. Petrie EJ, Sandow JJ, Lehmann WIL, Liang LY, Coursier D, Young SN, et al. Viral MLKL homologs subvert necroptotic cell death by sequestering cellular RIPK3. Cell Rep. 2019;28:3309–19.e3305.
10. Hildebrand JM, Kauppi M, Majewski IJ, Liu Z, Cox AJ, Miyake S, et al. A missense mutation in the MLKL brace region promotes lethal neonatal inflammation and hematopoietic dysfunction. Nat Commun. 2020;11:3150.
11. Muller T, Dewitz C, Schmitz J, Schroder AS, Brasen JH, Stockwell BR, et al. Necroptosis and ferroptosis are alternative cell death pathways that operate in acute kidney failure. Cell Mol Life Sci. 2017;74:3631–45.
12. Newton K, Dugger DL, Maltzman A, Greve JM, Hedehus M, Martin-McNulty B, et al. RIPK3 deficiency or catalytically inactive RIPK1 provides greater benefit than MLKL deficiency in mouse models of inflammation and tissue injury. Cell Death Differ. 2016;23:1565–76.
13. Rickard JA, Anderton H, Etemadi N, Nachbur U, Darding M, Peltzer N, et al. TNFR1-dependent cell death drives inflammation in Sharpin-deficient mice. Elife. 2014;3:e03464.
14. Rickard JA, O'Donnell JA, Evans JM, Lalaoui N, Poh AR, Rogers TW, et al. RIPK1 regulates RIPK3-MLKL driven systemic inflammation and emergency hematopoiesis. Cell. 2014;157:1175–88.
15. Degterev A, Hitomi J, Germscheid M, Ch'en IL, Korkina O, Teng X, et al. Identification of RIP1 kinase as a specific cellular target of necrostatins. Nat Chem Biol. 2008;4:313–21.
16. Holler N, Zaru R, Micheau O, Thome M, Attinger A, Valitutti S, et al. Fas triggers an alternative, caspase-8-independent cell death pathway using the kinase RIP as effector molecule. Nat Immunol. 2000;1:489–95.
17. He S, Wang L, Miao L, Wang T, Du F, Zhao L, et al. Receptor interacting protein kinase-3 determines cellular necrotic response to TNF-alpha. Cell. 2009;137:1100–11.
18. Zhang DW, Shao J, Lin J, Zhang N, Lu BJ, Lin SC, et al. RIP3, an energy metabolism regulator that switches TNF-induced cell death from apoptosis to necrosis. Science. 2009;325:332–6.
19. Murphy JM. The Killer Pseudokinase Mixed Lineage Kinase Domain-Like Protein (MLKL). Cold Spring Harbor Perspectives Biology. 2020;12:a036376.
20. Murphy JM, Czabotar PE, Hildebrand JM, Lucet IS, Zhang JG, Alvarez-Diaz S, et al. The pseudokinase MLKL mediates necroptosis via a molecular switch mechanism. Immunity. 2013;39:443–53.
21. Sun L, Wang H, Wang Z, He S, Chen S, Liao D, et al. Mixed lineage kinase domain-like protein mediates necrosis signaling downstream of RIP3 kinase. Cell. 2012;148:213–27.
22. Zhao J, Jitkaew S, Cai Z, Choksi S, Li Q, Luo J, et al. Mixed lineage kinase domain-like is a key receptor interacting protein 3 downstream component of TNF-induced necrosis. Proc Natl Acad Sci USA. 2012;109:5322–7.
23. Silke J, Rickard JA, Gerlic M. The diverse role of RIP kinases in necroptosis and inflammation. Nat Immunol. 2015;16:689–97.
24. Varfolomeev E, Blankenship JW, Wayson SM, Fedorova AV, Kayagaki N, Garg P, et al. IAP antagonists induce autoubiquitination of c-IAPs, NF-kappaB activation, and TNFalpha-dependent apoptosis. Cell. 2007;131:669–81.
25. Vince JE, Wong WW, Khan N, Feltham R, Chau D, Ahmed AU, et al. IAP antagonists target cIAP1 to induce TNFalpha-dependent apoptosis. Cell. 2007;131:682–93.
26. Lalaoui N, Boyden SE, Oda H, Wood GM, Stone DL, Chau D, et al. Mutations that prevent caspase cleavage of RIPK1 cause autoinflammatory disease. Nature. 2020;577:103–8.
27. Newton K, Wickliffe KE, Dugger DL, Maltzman A, Roose-Girma M, Dohse M, et al. Cleavage of RIPK1 by caspase-8 is crucial for limiting apoptosis and necroptosis. Nature. 2019;574:428–31.
28. Chen X, Li W, Ren J, Huang D, He WT, Song Y, et al. Translocation of mixed lineage kinase domain-like protein to plasma membrane leads to necrotic cell death. Cell Res. 2014;24:105–21.
29. Dondelinger Y, Declercq W, Montessuit S, Roelandt R, Goncalves A, Bruggeman I, et al. MLKL compromises plasma membrane integrity by binding to phosphatidylinositol phosphates. Cell Rep. 2014;7:971–81.
30. Hildebrand JM, Tanzer MC, Lucet IS, Young SN, Spall SK, Sharma P, et al. Activation of the pseudokinase MLKL unleashes the four-helix bundle domain to induce membrane localization and necroptotic cell death. Proc Natl Acad Sci USA. 2014;111:15072–7.
31. Petrie EJ, Birkinshaw RW, Koide A, Denbaum E, Hildebrand JM, Garnish SE, et al. Identification of MLKL membrane translocation as a checkpoint in necroptotic cell death using Monobodies. Proc Natl Acad Sci USA. 2020;117:8468–75.
32. Wang H, Sun L, Su L, Rizo J, Liu L, Wang LF, et al. Mixed lineage kinase domain-like protein MLKL causes necrotic membrane disruption upon phosphorylation by RIP3. Mol Cell. 2014;54:133–46.
33. Samson AL, Zhang Y, Geoghegan ND, Gavin XJ, Davies KA, Mlodzianoski MJ, et al. MLKL trafficking and accumulation at the plasma membrane control the kinetics and threshold for necroptosis. Nat Commun. 2020;11:3151.
34. Petrie EJ, Hildebrand JM, Murphy JM. Insane in the membrane: a structural perspective of MLKL function in necroptosis. Immunol Cell Biol. 2017;95:152–9.

35. Kaczmarek A, Vandenabeele P, Krysko DV. Necroptosis: the release of damage-associated molecular patterns and its physiological relevance. Immunity. 2013;38:209–23.
36. Liu ZG, Jiao D. Necroptosis, tumor necrosis and tumorigenesis. Cell Stress. 2019;4:1–8.
37. Pierdomenico M, Negroni A, Stronati L, Vitali R, Prete E, Bertin J, et al. Necroptosis is active in children with inflammatory bowel disease and contributes to heighten intestinal inflammation. Am J Gastroenterol. 2014;109:279–87.
38. Wu T, Dai Y, Xue L, Sheng Y, Xu L, Xue Y. Expression of receptor interacting protein 3 and mixed lineage kinase domain-like protein-key proteins in necroptosis is upregulated in ulcerative colitis. Ann Palliat Med. 2019;8:483–9.
39. Dannappel M, Vlantis K, Kumari S, Polykratis A, Kim C, Wachsmuth L, et al. RIPK1 maintains epithelial homeostasis by inhibiting apoptosis and necroptosis. Nature. 2014;513:90–94.
40. Takahashi N, Vereecke L, Bertrand MJ, Duprez L, Berger SB, Divert T, et al. RIPK1 ensures intestinal homeostasis by protecting the epithelium against apoptosis. Nature. 2014;513:95–99.
41. Moriwaki K, Balaji S, McQuade T, Malhotra N, Kang J, Chan FK. The necroptosis adaptor RIPK3 promotes injury-induced cytokine expression and tissue repair. Immunity. 2014;41:567–78.
42. Bozec D, Iuga AC, Roda G, Dahan S, Yeretssian G. Critical function of the necroptosis adaptor RIPK3 in protecting from intestinal tumorigenesis. Oncotarget. 2016;7:46384–400.
43. Alvarez-Diaz S, Dillon CP, Lalaoui N, Tanzer MC, Rodriguez DA, Lin A, et al. The pseudokinase MLKL and the kinase RIPK3 have distinct roles in autoimmune disease caused by loss of death-receptor-induced apoptosis. Immunity. 2016;45:513–26.
44. Wong WW, Vince JE, Lalaoui N, Lawlor KE, Chau D, Bankovacki A, et al. cIAPs and XIAP regulate myelopoiesis through cytokine production in an RIPK1- and RIPK3-dependent manner. Blood. 2014;123:2562–72.
45. Zhao Q, Yu X, Li M, Liu Y, Han Y, Zhang X, et al. MLKL attenuates colon inflammation and colitis-tumorigenesis via suppression of inflammatory responses. Cancer Lett. 2019;459:100–11.
46. Zhang J, Qin D, Yang YJ, Hu GQ, Qin XX, Du CT, et al. MLKL deficiency inhibits DSS-induced colitis independent of intestinal microbiota. Mol Immunol. 2019;107:132–41.
47. Cook WD, Moujalled DM, Ralph TJ, Lock P, Young SN, Murphy JM, et al. RIPK1- and RIPK3-induced cell death mode is determined by target availability. Cell Death Differ. 2014;21:1600–12.
48. Newton K, Dugger DL, Wickliffe KE, Kapoor N, de Almagro MC, Vucic D, et al. Activity of protein kinase RIPK3 determines whether cells die by necroptosis or apoptosis. Science. 2014;343:1357–60.
49. Ernst M, Preaudet A, Putoczki T. Non-invasive assessment of the efficacy of new therapeutics for intestinal pathologies using serial endoscopic imaging of live mice. J Vis Exp. 2015;97:52383.
50. Neumann PA, Koch S, Hilgarth RS, Perez-Chanona E, Denning P, Jobin C, et al. Gut commensal bacteria and regional Wnt gene expression in the proximal versus distal colon. Am J Pathol. 2014;184:592–9.
51. Merlano MC, Granetto C, Fea E, Ricci V, Garrone O. Heterogeneity of colon cancer: from bench to bedside. ESMO Open. 2017;2:e000218.
52. Neufert C, Becker C, Neurath MF. An inducible mouse model of colon carcinogenesis for the analysis of sporadic and inflammation-driven tumor progression. Nat Protoc. 2007;2:1998–2004.
53. Tanaka T, Suzuki R, Kohno H, Sugie S, Takahashi M, Wakabayashi K. Colonic adenocarcinomas rapidly induced by the combined treatment with 2-amino-1-methyl-6-phenylimidazo[4,5-b]pyridine and dextran sodium sulfate in male ICR mice possess beta-catenin gene mutations and increases immunoreactivity for beta-catenin, cyclooxygenase-2 and inducible nitric oxide synthase. Carcinogenesis. 2005;26:229–38.
54. Wirtz S, Neufert C, Weigmann B, Neurath MF. Chemically induced mouse models of intestinal inflammation. Nat Protoc. 2007;2:541–6.
55. Sai K, Parsons C, House JS, Kathariou S, Ninomiya-Tsuji J. Necroptosis mediators RIPK3 and MLKL suppress intracellular Listeria replication independently of host cell killing. J Cell Biol. 2019;218:1994–2005.
56. Moser AR, Pitot HC, Dove WF. A dominant mutation that predisposes to multiple intestinal neoplasia in the mouse. Science. 1990;247:322–4.
57. Gunther C, Martini E, Wittkopf N, Amann K, Weigmann B, Neumann H, et al. Caspase-8 regulates TNF-alpha-induced epithelial necroptosis and terminal ileitis. Nature. 2011;477:335–9.
58. Patel S, Webster JD, Varfolomeev E, Kwon YC, Cheng JH, Zhang J, et al. RIP1 inhibition blocks inflammatory diseases but not tumor growth or metastases. Cell Death Differ. 2020;27:161–75.
59. Wang T, Perera ND, Chiam MDF, Cuic B, Wanniarachchillage N, Tomas D, et al. Necroptosis is dispensable for motor neuron degeneration in a mouse model of ALS. Cell Death Differ. 2020;27:1728–39.
60. Webster JD, Kwon YC, Park S, Zhang H, Corr N, Ljumanovic N, et al. RIP1 kinase activity is critical for skin inflammation but not for viral propagation. J Leukoc Biol. 2020;107:941–52.
61. Gobbetti T, Berger SB, Fountain K, Slocombe T, Rowles A, Pearse G, et al. Receptor-interacting protein 1 kinase inhibition therapeutically ameliorates experimental T cell-dependent colitis in mice. Cell Death Dis. 2020;11:220.
62. Nguyen PM, Dagley LF, Preaudet A, Lam N, Giam M, Fung KY, et al. Loss of Bcl-G, a Bcl-2 family member, augments the development of inflammation-associated colorectal cancer. Cell Death Differ. 2020;27:742–57.
63. Zhao XM, Chen Z, Zhao JB, Zhang PP, Pu YF, Jiang SH, et al. Hsp90 modulates the stability of MLKL and is required for TNF-induced necroptosis. Cell Death Dis. 2016;7:e2089.
64. Vanden Berghe T, Hulpiau P, Martens L, Vandenbroucke RE, Van Wonterghem E, Perry SW, et al. Passenger mutations confound interpretation of all genetically modified congenic mice. Immunity. 2015;43:200–9.
65. Newton K, Sun X, Dixit VM. Kinase RIP3 is dispensable for normal NF-kappa Bs, signaling by the B-cell and T-cell receptors, tumor necrosis factor receptor 1, and toll-like receptors 2 and 4. Mol Cell Biol. 2004;24:1464–9.
66. Mielke L, Preaudet A, Belz G, Putoczki T. Confocal laser endomicroscopy to monitor the colonic mucosa of mice. J Immunol Methods. 2015;421:81–88.